Synthesis of Magnetically-Responsive Photocatalytic CuBTC Metal-Organic-Frameworks (MOFs) for Degradation of Organic Dyes

Peng Zikang (4S1), Ng Yan Bin Lucas (4S3), Eun Chin Sze Gerald (4S3)

01-40

Abstract

CuBTC (Copper benzene-1,3,5-tricarboxylate) is a Metal Organic Framework (MOF) which has the potential to degrade azo dyes from wastewater via photocatalysis. In this study, non-magnetic and magnetic CuBTC were synthesized via intercalation and crystallization. CuBTC MOF displays enhanced photocatalytic activity under visible light, with photodegradation of methyl orange and direct red further catalyzed by the addition of hydrogen peroxide. Magnetization of CuBTC doped with mercapto-acetic acid (MAA) as a capping agent reduced agglomeration and further enhanced dye degradation efficacy. The band gap of magnetic CuBTC and non-magnetic CuBTC MOF synthesized were 1.98eV and 2.03 eV respectively, which are both lower than that of conventional catalysts such as titanium dioxide (TiO_2) and zinc oxide (ZnO). Hence, both magnetic and non-magnetic CuBTC MOF are able to harness visible light and outperformed both TiO_2 and ZnO under visible light irradiation, with magnetic CuBTC removing close to 100% of both dyes in the presence of hydrogen peroxide. Hence, magnetic CuBTC MOF is a promising alternative to conventional photocatalysts in degrading dyes.

1. Introduction

The textile industry is worth around US$1 trillion worldwide and makes up 7% of the total world exports (Desore & Narula, 2017). The most common dyes used in the textile industry are azo dyes which make up 60-70% of all dyes used (Wakelyn, 2007). The continuous usage of azo dyes has been responsible for an extensive list of environmental impacts. The main damages caused by the textile industry to the environment result mainly from the discharge of untreated effluents containing azo dyes into the water bodies (Bhatia, 2017), which normally constitute 80% of the total emissions produced by this industry (Wang, 2016). The colour associated with textile dyes not only causes aesthetic damage to the water bodies (Setiadi, Andriani & Erlania 2006), and also prevents the penetration of light through water (Hassan & Carr, 2018), which leads to a reduction in the rate of photosynthesis (Imran et al., 2015) and dissolved oxygen levels, affecting

the entire aquatic biota (Hassan & Carr, 2018). The textile dyes also act as toxic, mutagenic and carcinogenic agents (Aquino et al., 2014).

Azo dyes are very difficult to break down as it consists of one or more azo bonds (–N=N-) in association with one or more aromatic systems (Thi, Ngoc, Manh, & Kim, 2010). The removal of azo dyes from wastewater is a challenge to the textiles industries because the azo dyes are difficult to destroy by biological and conventional chemical treatments due to their toxicity and stability. For removal of azo dyes from industrial wastewater, adsorption has shown to be one of the most effective methods and activated carbon is the preferred adsorbent because of its efficiency, capacity and scalability for commercial usage (Mattson & Mark, 1971). However, adsorption using activated carbon does not degrade the dye and adsorptive properties of the activated carbon will gradually become weak after continuous dye removal (Wawrzkiewicz, 2012). Therefore, a high cost is incurred due to the necessity of disposal and incineration (Schrank, dos Santos, Souza & Souza, 2007).

In recent years, photodegradation has emerged as an efficient and green method to degrade dyes from wastewater. One of the most common photocatalyst used is titanium dioxide (TiO_2) nanoparticles. TiO_2, under ultraviolet (UV) light, is able to photocatalyse the decomposition of organic pollutants by light-induced electron/hole pairs and highly oxidising hydroxyl and superoxide radical anions (Saquib & Muneer, 2003). However, due to the large band gap energy of TiO_2 (around 3.2 eV), it is only responsive to UV light which accounts for only about 5% of the solar spectrum (Moma & Baloyi, 2018), reducing its effectiveness in a large-scale setting. Therefore, there is a need to develop a quick and efficient method for the synthesis of an inexpensive photocatalyst that works under visible light irradiation.

The CuBTC MOF is a type of Metal-Organic-Framework (MOF) which has photocatalytic properties. Metal-Organic-Frameworks (MOFs) have emerged as an extensive class of crystalline materials with ultrahigh porosity and enormous internal surface areas. Cu-BTC is a neutral coordination polymer composed of dimeric cupric tetracarboxylate units.

Copper-benzenecarboxylate units form a face-centered crystal lattice of *Fm3m* symmetry, which has a complex three-dimensional channel system, forming extensive pore networks (Figure 1) (Vishnyakov, Ravikovitch, Neimark, Bulow, & Wang, 2013). It has a moderate band gap (2.0 eV) and is potentially able to harness visible light for photodegradation. Furthermore, it is possible to magnetise CuBTC to enhance its reusability.

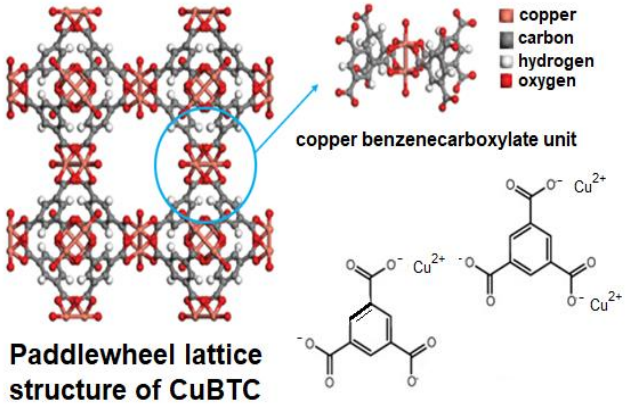

Figure 1: Chemical structure of CuBTC MOF

As with the case with other MOFs, Cu-BTC also has been extensively studied for gaseous adsorption (Li et al., 2019). To date, there have been limited studies on the use of CuBTC to degrade dyes, especially azo dyes. Hence, this study aims to synthesize CuBTC via a simple and facile intercalation and crystallization method and to investigate its effectiveness in degrading methyl orange and direct red dyes.

2. Objectives and Hypothesis

This study aims to synthesize non-magnetic CuBTC and magnetic CuBTC via intercalation and crystallization, investigate the effects of visible light, H_2O_2 and presence of magnetite on the photodegradation capabilities of CuBTC on azo dyes (methyl orange and direct red) and compare the effectiveness of non-magnetic CuBTC and magnetic CuBTC with conventional photocatalysts (zinc oxide and titanium dioxide).

It is hypothesized that CuBTC can be synthesized via intercalation and crystallization, the presence of visible light, magnetite and H_2O_2 will improve photodegradation of dyes and magnetic CuBTC will show higher degradation capabilities compared to zinc oxide and titanium dioxide.

3. Materials and Methods

3.1. Materials

Copper (II) nitrate was purchased from GCE Chemicals. Trimesic acid (H_3BTC), magnetite, mercapto-acetic acid (MAA), methyl orange and direct red were procured from Sigma Aldrich.

3.2. Methods

3.2.1 Synthesis of copper (II) benzene 1,3,5-tricarboxylate (CuBTC) MOF

1.82g of $Cu(NO_3)_2$ and 0.875g of H_3BTC were dissolved in 100ml of deionized water in separate beakers. The solution of H_3BTC was then added to the dissolved $Cu(NO_3)_2$, with a constant flow rate of 1ml min^{-1}, and then topped up to 250ml with absolute ethanol and left to stir for 8 hours. The reaction leading to the formation of CuBTC is shown in equation 1.

$$3Cu(NO_3)_2 + 2H_3BTC + 3H_2O \rightarrow [\mathbf{Cu_3BTC_2}].3H_2O + 6HNO_3 \qquad \text{Eq 1}$$

The suspension was then centrifuged and the residue was washed with absolute ethanol, before leaving it to dry in the oven at 70^{o}C until constant mass.

3.2.2 Magnetization of CuBTC MOF

0.50g of magnetite powder was added to 1.0ml of mercapto-acetic acid (MAA) and dispersed in 9.0ml of absolute ethanol. The suspension was shaken for 24 hours at 150rpm, and then centrifuged. The residue was washed and collected. 0.5g of MAA-functionalized magnetite was added to the synthesized CuBTC and dispersed in 100ml of absolute ethanol and the suspension was sonicated for 2 hours. The resultant magnetic CuBTC was washed and dried in the oven at 70^{o}C until constant mass.

3.2.3 Determination of effectiveness of CuBTC MOF in degrading dyes

0.050g of magnetic and non-magnetic CuBTC MOF and varying volumes of 6% hydrogen peroxide were added to 20 ml of 25 ppm dye solution and stirred for 24 hours in the dark or under the irradiation of visible light. The magnetic CuBTC MOF was separated using a magnet while the non-magnetic CuBTC MOF was separated by centrifugation. The concentration of dye remaining in the supernatant was measured using a UV-Vis Spectrophotometer at λ=464 nm for methyl orange and λ=526 nm for direct red. A control with no CuBTC MOF and hydrogen peroxide was included in the set up. The experiments were repeated with conventional

photocatalysts, titanium dioxide and zinc oxide for comparison. Five replicates were conducted for each photocatalyst. The following formula was used to calculate the percentage of dye removed:

$$P_d = \frac{C_i - C_f}{C_i} \times 100\%$$

where
P_d = Percentage of dye removed
C_i = Initial concentration of dye in ppm
C_f = Final concentration of dye in ppm

3.2.4 Investigating the effect of varying concentrations of H_2O_2, presence of visible light irradiation and presence of magnetite on dye degradation efficiencies

Different volumes (0.5 to 2.0 ml) of hydrogen peroxide were added to separate samples of non-magnetic and magnetic CuBTC MOF and photodegradation was carried out as described in section 3.2.3. Five replicates were performed for each concentration of H_2O_2 for both non-magnetic and magnetic CuBTC MOF, which were carried out both under visible light irradiation and in the dark.

4. Results and discussion

4.1 Effect of magnetization of CuBTC MOF on percentage removal of dyes

Figure 2 shows the effect of magnetising CuBTC MOF with magnetite pre-treated with capping agent (MAA). Magnetizing CuBTC MOF allowed the MOF to degrade a significantly larger percentage of methyl orange (97.40%) as well as direct red 80 dye (99.12%) as compared to non-magnetic CuBTC MOF. A p-value of 0.013 was obtained from the Mann-Whitney Test (significance level of 0.05) conducted on the data of both direct red 80 and methyl orange adsorption, suggesting that the magnetite treated with capping agents significantly enhances the photocatalyst's performance.

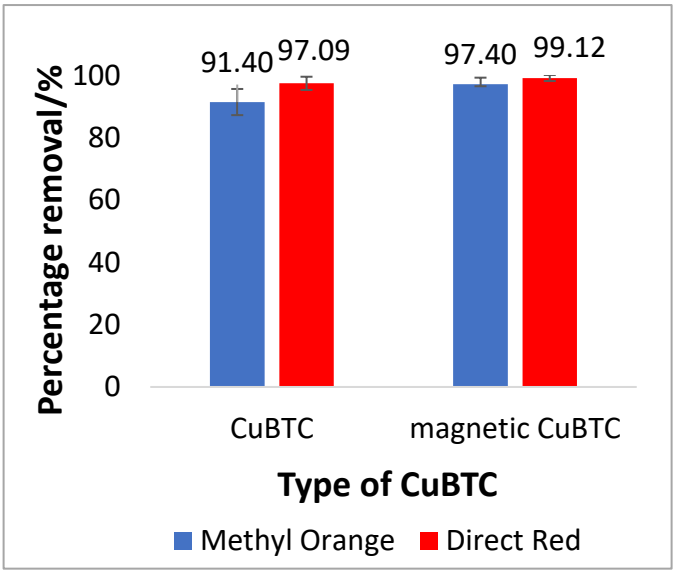

Figure 2: Photodegradation of azo dyes by magnetic and non-magnetic CuBTC

4.2 Characterization of synthesized CuBTC MOF by Scanning Electron Microscope (SEM)

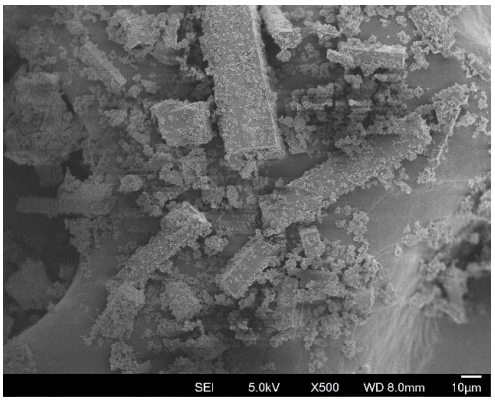

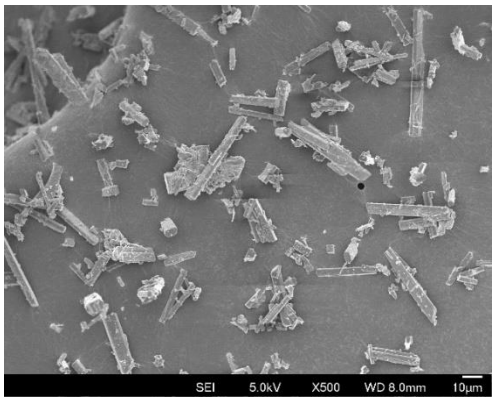

Figure 3a: SEM image of non-magnetic CuBTC **Figure 3b**: SEM image of magnetic CuBTC

Non-magnetic CuBTC MOF (Figure 3a) shows evidence of agglomeration on the crystal surface and the observation is in agreement with that synthesised by Fang, Bueken, De Vos and Fischer (2015). This is caused by high surface energy that leads to inhomogeneous particle packing and thus agglomeration (Ploetz, Engelke, Lachelt & Wuttke, 2020). Agglomeration inside the MOF can reduce the charge transfer at the associated interface, increase the band gap of CuBTC MOF, and accelerate non-radiative electron–hole recombination by a factor of 3, which accounts for the poorer degradation of dyes (Wei, Zhou, Fang & Long, 2018).

On the other hand, SEM image of magnetic CuBTC MOF reveals distinct and regular shaped crystals (Figure 3b), which was also in agreement by other researchers (Fang et.al., 2015). This is due to iron in magnetite binding to the dangling carboxylic acid groups in CuBTC MOF with surface defects and this allows for more complete crystal growth, increasing the MOF's pore size and overall surface area. MAA used to dope magnetic CuBTC also helps prevent agglomeration unlike non-magnetic CuBTC. This is due to MAA serving as a capping agent which prevents magnetite nanoparticles from agglomerating while maintaining high total surface area for photocatalytic acitivty.

4.3 Effect of presence of visible light and hydrogen peroxide on dye degradation

To confirm the photocatalytic capability of the CuBTC MOF, dye degradation experiments were conducted both in the dark and under visible light irradiation. Both the magnetic and non-magnetic CuBTC MOF were able to remove at least 10% of dyes in the dark, suggesting that the MOFs could remove dye by adsorption. Under visible light irradiation, both magnetic and non-magnetic CuBTC MOF had a significantly higher percentage removal of direct red and methyl

orange as compared to similar setups in the absence of visible light. This highlights that both adsorption and photodegradation in the presence of visible light removes more dyes than adsorption under dark conditions alone.

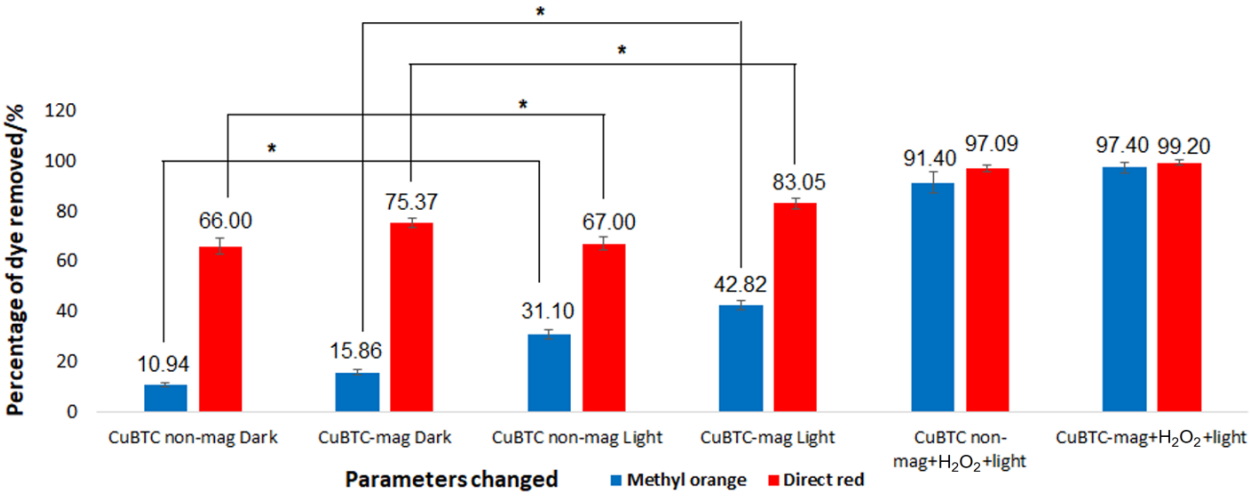

Figure 4: Comparison of the effects of the presence of light and addition of H_2O_2 on the percentage removal of dyes. * denotes statistical significance based on Mann Whitney U Test at a significance level of 0.05

When visible light is irradiated on the surface of the CuBTC MOF, CuBTC releases electrons which react with the surrounding O_2 and H_2O molecules to produce the superoxide anion and hydroxyl radicals, which are able to degrade the azo dyes on top of adsorption. The addition of H_2O_2 increases the production of these hydroxyl radicals by not only reacting with the electrons produced, but also the superoxide anions to produce more hydroxyl radicals (Tseng, Juang & Huang, 2012), as shown in equations 2 and 3, hence improving the percentage of dye removed as compared to without the addition of H_2O_2.

$$H_2O_2 + e^- \longrightarrow \bullet OH + OH^- \qquad \text{eq 2}$$

$$H_2O_2 + O_2^{\bullet -} \longrightarrow \bullet OH + OH^- + O_2 \qquad \text{eq 3}$$

4.4. Effect of volume of H_2O_2 on percentage of dye removed

Figure 5a shows that when the volume of H_2O_2 increases from 0 to 1.5ml, the percentage of methyl orange removed increases from 15.86% to 91.40% while the percentage of direct red removal increases from 75.00% to 97.09% for non-magnetic CuBTC MOF. This is because when the volume H_2O_2 is increased, more superoxide anions react with H_2O_2 to produce more hydroxyl radicals, which degrade azo dyes more efficiently. The same trend applies for magnetic CuBTC

MOF. Hydroxyl radicals generated attack the azo group (-N=N-) in methyl orange and direct red, cleaving the bond, leading to dye degradation.

Yet, when volume of H_2O_2 was further increased to 2.0ml, the percentage of methyl orange and direct red removal by non-magnetic CuBTC MOF decreases to 88.81% and 95.94% respectively. H_2O_2 is a hydroxyl radical scavenger (Tseng, Juang & Huang, 2012), suggesting excess H_2O_2 causes the amount of hydroxyl radicals produced to decrease instead (Equations 4 and 5).

$$H_2O_2 + {}^{\bullet}OH \longrightarrow H_2O + OH_2{}^{\bullet} \qquad \text{eq 4}$$

$$HO_2{}^{\bullet} + {}^{\bullet}OH \longrightarrow H_2O + O_2 \qquad \text{eq 5}$$

Therefore, through analysis of the graph, it can be concluded that the ideal volume of H_2O_2 for both non-magnetic and magnetic CuBTC MOF is 1.5ml as the percentage of dye removed is at its peak.

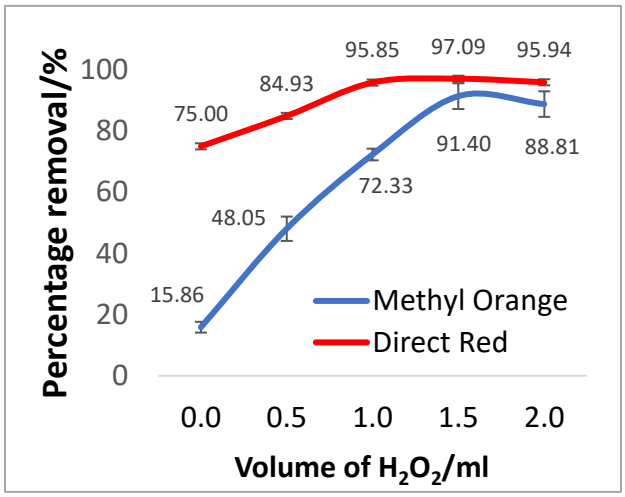

Figure 5a: Effect of volume of H_2O_2 on dye degradation by non-magnetic CuBTC MOF

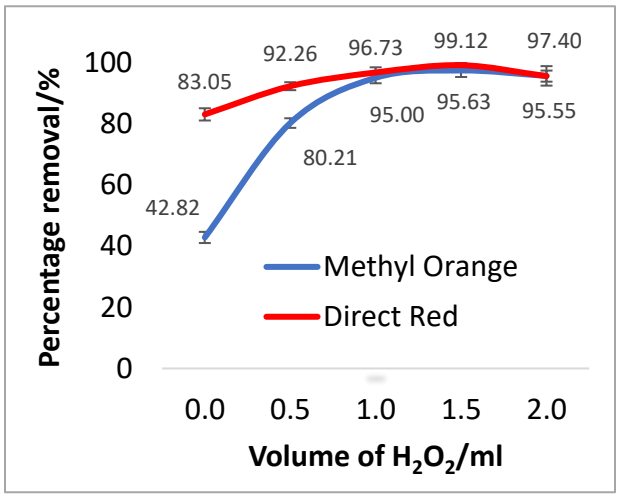

Figure 5b: Effect of volume of H_2O_2 on dye degradation by magnetic CuBTC MOF

4.5 Comparison of photocatalytic degradation performance of CuBTC-MOF with other conventional photocatalysts

Comparing CuBTC MOF with conventional photocatalysts (ZnO and TiO_2) under visible light, both magnetic CuBTC and non-magnetic CuBTC MOF showed higher percentages of dye degradation than both zinc oxide and titanium dioxide (Figure 6).

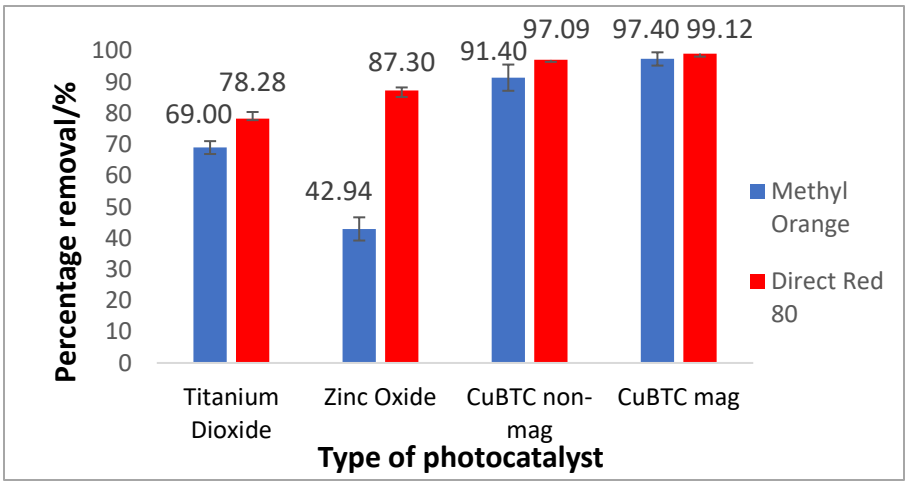

Figure 6: Comparison between percentage of dye removed by different photocatalysts under visible light and in the presence of 1.5 ml of H_2O_2

The band gap of semiconductor photocatalysts is a crucial factor in determining their photocatalytic efficiency, since it is an indicator of how much energy from the visible light region they could capitalize. Zinc oxide and titanium dioxide both have high band gaps of 3.2 eV (Dodd, Mckinley, Tsuzuki & Saunders, 2009), which only allowed them to catalyze the photodegradation reactions efficiently in UV-light but not visible light. However, the CuBTC MOF synthesized in this study was determined to have a band gap of 1.98 eV (Figure 7b) for magnetic CuBTC MOF and 2.03 eV (Figure 7a) for non-magnetic MOF, which are both lower than zinc oxide and titanium dioxide. This means that both CuBTC MOFs were able to harness light from visible light spectra more effectively and hence outperform the conventional catalysts.

Another interesting observation is that magnetic CuBTC MOF is more effective in degrading both dyes than non-magnetic CuBTC MOF. This is due to the magnetic CuBTC MOF having a lower band gap than non-magnetic CuBTC MOF (Figure 7(a) and (b)).

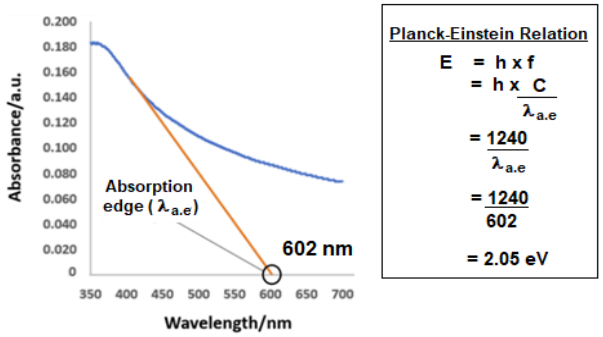

Figure 7a: Calculation of band gap (E_g) for non-magnetic CuBTC

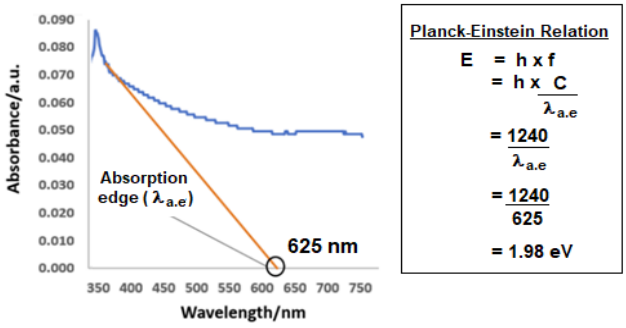

Figure 7b: Calculation of band gap (E_g) for magnetic CuBTC

5. Conclusion and future studies

Magnetic and non-magnetic CuBTC MOF were synthesized via intercalation and crystallization. Magnetization of CuBTC with MAA-functionalized Fe_3O_4 enhanced the degradation of both methyl orange and direct red. CuBTC displayed photocatalytic activity under visible light and presence of H_2O_2 improves the percentage of dyes degraded. The optimum volume of H_2O_2 which results in highest percentage of dyes degraded is 1.5 ml for both types of CuBTC MOF. Under visible light irradiation and the presence of 1.5ml of H_2O_2, magnetized CuBTC is able to degrade up to 99% of direct red and 97% of methyl orange. When compared to conventional photocatalysts, non-magnetic CuBTC and magnetic CuBTC have a lower band gap and hence better degradation capabilities. Magnetizing CuBTC MOF shows great promise as an effective photocatalyst for degrading azo dyes from wastewater. As CuBTC MOF is able to function effectively in the presence of visible light unlike conventional catalyst such as titanium dioxide which requires UV, the use of it could potentially lower cost of operation.

In the future, the dye residue of both methyl orange and direct red could be analysed with mass spectrometry to better understand the dye mechanism by CuBTC MOF. Rate of dye degradation by both types of CuBTC MOF could be determined. Degradation of other types of organic pollutants like ibuprofen and malathion by CuBTC MOF could also be explored. Finally, a prototype (Figure 8) which degrades dyes in wastewater using magnetic CuBTC MOF could be built and tested. Magnetic CuBTC MOF will be placed in a transparent reactor tank to allow it to harness visible light for degradation. An electromagnet will be used to maneuver the magnetic CuBTC MOF and to facilitate the separation of the catalyst from wastewater after treatment. The colour intensity of wastewater will be monitored by a colorimetric datalogger to monitor when the dye degradation is complete.

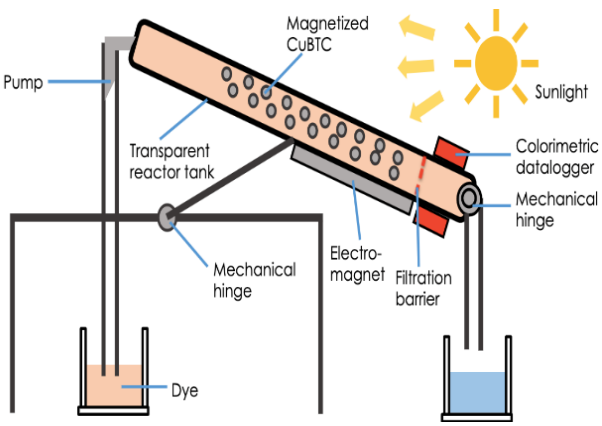

Figure 8: Proposed model of photocatalytic reactor for dye degradation

References

Aquino, J.M., Rocha-Filho, R.C., Ruotolo, L.A., Bocchi, N., & Biaggio, S.R. (2014). Electrochemical degradation of a real textile wastewater using β-PbO2 and DSA® anodes. *Chemical Engineering Journal*, *251*, 138-145. DOI: https://doi.org/10.1016/j.cej.2014.04.032

Bhatia, S.C. (2017). *Pollution Control in Textile Industry*. Woodhead Publishing India Ptv. Ltd. Retrieved from

https://books.google.com.sg/books/about/Pollution_Control_in_Textile_Industry.html?id=fmQ-DwAAQBAJ&printsec=frontcover&source=kp_read_button&redir_esc=y#v=onepage&q&f=false

Desore, A., & Narula, S.A. (2017). An overview on corporate response towards sustainability issues in textile industry. *Environmental Developmental and Sustainability*, *20*(4), 1439-1459.

DOI: https://doi.org/10.1007/s10668-017-9949-1

Dodd A., Mckinley A., Tsuzuki T. & Saunders. M. (2009) Tailoring the photocatalytic activity of nanoparticulate zinc oxide by transition metal oxide doping, *Materials Chemistry and Physics*, *114*(1), 382-386. DOI: https://doi.org/10.1016/j.matchemphys.2008.09.041

Fang, Z. L., Bueken, B., De Vos, D., & Fischer, R. A. (2015) Defect Engineered Metal-Organic-Frameworks. *Angew. Chem. Int. Ed.*, *54*, 7234 – 7254

DOI: https://doi.org/10.1002/anie.201411540

Gerischer, H. (1993). Photo electrochemical catalysis of the oxidation of organic molecules by oxygen on small semiconductor with TiO_2 as an example. *Electrochichima Acta*, *38*(1), 3-9

DOI:https://doi.org/10.1016/0013-4686(93)80003-I

Hassan, M.M., & Carr, C.M. (2018) A critical review on recent advancements of the removal of reactive dyes from dyehouse effluent by ion-exchange adsorbents. *Chemosphere*, *209*, 201-219

DOI: https://doi.org/10.1016/j.chemosphere.2018.06.043

Imran, M., Crowley, D.E., Khalid, A., Hussain, S., Mumtaz, M.W., & Arshad, M. (2014). Microbial biotechnology for decolorization of textile wastewaters. *Reviews in Environmental Science and Bio/Technology*, *14*, 73-92. DOI: https://doi.org/10.1007/s11157-014-9344-4

Lin, K.Y.A., Chang, H.A., & Hsu, C.J. (2015). Iron-based metal organic framework, MIL-88A, as a heterogeneous persulfate catalyst for decolorization of Rhodamine B in water, *RSC Advances*, *41*. DOI: https://doi.org/10.1039/C5RA01447F

Mattson, J.S. & Mark, H.B. (1971). *Activated Carbon*, Marcel Dekker, New York.

Moma J., & Baloyi J. (2018). *Modified Titanium Dioxide for Photocatalytic Applications*. *IntechOpen*. DOI: https://doi.org/10.5772/intechopen.79374

Ploetz E., Engelke H., Lachelt U, & Wuttke S. (2020) The Chemistry of Reticular Framework Nanoparticles: MOF, ZIF, and COF Materials. *Advanced Functional Materials*, 1909062 DOI: https://doi.org/10.1002/adfm.201909062

Saquib, M., & Muneer, M. (2003) TiO2-mediated photocatalytic degradation of a triphenylmethane dye (gentian violet), in aqueous suspension. *Dyes and Pigments 56*, 37-49

DOI: https://doi.org/10.1016/S0143-7208(02)00101-8

Schrank, S.G., dos Santos, J.N.R., Souza, D.S., & Souza, E.E.S. (2007) Decolourisation effects of Vat Green 01 textile dye and textile wastewater using H_2O_2/UV process. *Journal of Photochemistry and Photobiology A Chemistry*, *186*(2) 125-129.

DOI: https://doi.org/10.1016/j.jphotochem.2006.08.001

Setiadi, T., Andriani, Y., & Erlania, M. (2005) Treatment of textile wastewater by a combination of anaerobic and aerobic processes: A denim processing plant case. *Southeast Asian Water Environment 1*, 159-166. DOI: https://doi.org/10.2166/9781780402987

Thi, D.N., Ngoc, H.P., Manh, H.D., & Kim, T.N. (2011) Magnetic Fe_2MO_4 (M:Fe, Mn) activated carbons: Fabrication, characterization and heterogeneous Fenton oxidation of methyl orange. *Journal of Hazardous Materials*, *185*(2-3), 653-661. DOI: https://doi.org/10.1016/j.jhazmat.2010.09.068

Tseng D.H., Juang L.C. & Huang H.H. (2012) Effect of Oxygen and Hydrogen Peroxide on the Photocatalytic Degradation of Monochlorobenzene in TiO2 Aqueous Suspension. *International Journal of Photoenergy, 2012.* DOI: https://doi.org/10.1155/2012/328526

Vishnyakov A., Ravikovitch P.I., Neimark A.V., Bulow M., Wang Q.M. (2003) Nanopore Structure and Sorption Properties of Cu−BTC Metal−Organic Framework. *Nano Letters*, *3*(6), 713-718 DOI: https://doi.org/10.1021/nl0341281

Wakelyn, P.J. (2007). Health and safety issues in cotton production and processing. *Cotton Science and Technology*, 460-483. DOI: https://doi.org/10.1533/9781845692483.3.460

Wang, D.M. (2016). Environmental protection in clothing industry. *Sustainable Development*, 729-735. DOI: https://doi.org/10.1142/9789814749916_0076

Wawrzkiewicz, M. (2012) Anion Exchange Resins as Effective Sorbents for Acidic Dye Removal from Aqueous Solutions and Wastewaters. *Solvent Extraction and Ion Exchange, 30*(5), 507-523. DOI: https://doi.org/10.1080/07366299.2011.639253

Wei Y., Zhou Z., Fang W.H., Long R. (2018) Grain boundary Facilitates Photocatalytic Reaction in Rutile TiO2 Despite Fast Charge Recombination: A Time Domain *ab Initio* Analysis. *J. Phys. Chem. Lett, 9*(19), 5884-5889. DOI: https://doi.org/10.1021/acs.jpclett.8b02761